
Deep feedforward functionality by equilibrium-point control in a shallow recurrent network

Anonymous Author(s)

Affiliation

Address

email

Abstract

1 Recurrent neural network based machine learning systems are typically employed
2 for their sequential functionality in handling time-varying signals, such as for
3 speech processing. However, neurobiologists find recurrent connections in the
4 vision system and debate about equilibrium-point control in the motor system.
5 Thus, we need a deeper understanding of how recurrent dynamics can be exploited
6 to attain combinational stable-input stable-output functionality. Here, we study
7 how a simplified Cohen-Grossberg neural network model can realize combinational
8 multi-input Boolean functionality. We place our problem within the discipline of
9 algebraic geometry, and solve a special case of it using piecewise-linear algebra.
10 We demonstrate a connectance-efficient realization of the parity function as a
11 proof-of-concept. Small-scale systems of this kind can be easily built, say for
12 hobby robotics, as a network of two-terminal devices of resistors and tunnel diodes.
13 Large-scale systems may be energy-efficiently built as an interconnected network
14 of multi-electrode nanoclusters with non-monotonic transport mechanisms.

15 1 Introduction

16 Shallow recurrent neural networks are being investigated for more context-aware object recognition
17 [25] and brain-like behaviour [23]. They can be more compact (by trading space for time) and are a
18 naturally robust alternative to deep neural networks (which are easily fooled by input perturbations
19 or transformations [18, 29, 1]) when the role of recurrent dynamics is not to produce time-varying
20 output but instead to produce transient (hidden) state-dynamics that facilitate deep, robust and
21 transformation-invariant fixed-input fixed-output functionality. To better engineer such dynamics,
22 we shall study equilibrium-point control, which can be defined as the process of steering to a target
23 in state-space by fixing the input signal, instead of driving it by a continuously varying input signal.
24 Historically, equilibrium-point control [14, 5] was first formulated to provide a plausible solution
25 to the degrees of freedom problem in motor control [3], that is, we mentally represent intermediate
26 destination points rather than a continuum of velocity information required to execute a movement.

27 Here, we shall focus on using equilibrium-point control to realize multi-input Boolean functionality,
28 in particular the parity function, which is a canonical proxy for nonlinear classification. Theoretical
29 results in circuit complexity are known already for realizing Boolean functionality out of feedforward
30 neural networks, with weighted-sum thresholded binary-output neurons [35]. It has been shown that
31 arbitrary N -input Boolean functions can be realized in depth-3 feedforward networks with fewer
32 neurons ($m = \mathcal{O}(2^{N/2})$) instead of the $\mathcal{O}(2^N)$ in total required for depth-2). However, with the
33 advent of nanoelectronics, the size of an artificial neuron has been downscaled to such an extent
34 that it is rather the interconnect wiring that now occupies a greater area in chip design. Thus for a
35 fully-connected deep network, the area scales as the number of interconnects $m^2 = \mathcal{O}(2^N)$. Such a

36 $\mathcal{O}(2^N)$ scaling law was earlier obtained by Shannon [34] for realizing arbitrary N -input Boolean
 37 functions by an interconnection of input-controlled switches (or equivalently a feedforward network
 38 of 2-input Boolean gates). Thus, unless we employ higher-order neurons [16], we can say that
 39 a *Shannon bottleneck* limits the maximum N -input Boolean logic realizable in a given area by
 40 (nanoscale) feedforward networks. We aim to circumvent this Shannon bottleneck by employing
 41 recurrent physical networks. It is known that certain combinational logic functions can be realized
 42 by fewer logic gates in a cyclic network than in an acyclic network [31], and with analog signal
 43 processing the improvement factor could be even higher.

44 In the following section, we introduce a state-space model formalism to study equilibrium-point
 45 control, and commit to a physically realizable model, and discuss how a general solution for its
 46 equilibrium points is a difficult problem in algebraic geometry. Thus, we proceed to idealize the non-
 47 monotonic output of the physical system as a piecewise-linear function and solve for the equilibrium
 48 points. Finally, a piecewise-quadratic Lyapunov function is obtained for stability analysis and
 49 conditions for a unique equilibrium-point are provided.

50 After the theory, in the results section, we provide a connectance-efficient realization of the parity
 51 function. The discussion section puts our results into a broader context and offers avenues for further
 52 research. Our objective here is to work at the intersection of nonlinear dynamical systems, neural
 53 networks, unconventional neuromorphic hardware, cyclic Boolean circuits, piecewise-linear control
 54 systems, and algebraic geometry.

55 2 Theory

56 2.1 State-space model

57 For equilibrium-point control, in general we have an input vector \mathbf{x} , a state $s_i(t)$ for $i = 1 : N$, and
 58 an output y obtained from a system of equations

$$\dot{s}_i(t) = F_i(\mathbf{s}(t), \mathbf{x}), y = \lim_{t \rightarrow \infty} G(\mathbf{s}(t)). \quad (1)$$

59 In this paper, we commit to a physically realizable recurrent network with voltage nodes s_i from
 60 $i = 1 : N$, with a capacitive time-constant τ_i , using resistors (of a constant conductance f_{ij}) and
 61 tunnel diodes (of a voltage-dependent conductance $G_i(s_i)$) as shown in Fig. 1, yielding a state-space
 62 model of the form

$$\tau_i \dot{s}_i = x_i - \sum_{j \neq i} f_{ij}(s_i - s_j) - G_i(s_i), y = G_1(\hat{s}_1) \quad (2)$$

63 where $f_{ij} \geq 0$, G_i is a nonlinear passive function such that $G_i(s)s \geq 0$ and $\hat{s}_1 \equiv \lim_{t \rightarrow \infty} s_1(t)$ is
 64 the stable equilibrium-point if one exists (note: $y(\mathbf{x})$ can be multi-valued and depend on the basin of
 65 attraction that the initial state $\mathbf{s}(0)$ lies in). Brain-scale systems of this kind may be realized by an
 66 interconnected network of nanoclusters with non-monotonic transport mechanisms as proposed in
 67 [24, Chapter 5]. However, finding suitable network parameters that result in practical functionality
 68 remains a challenge. Note that, although not the focus of this work, Eq. (2) can also represent
 69 state-space models with noisy rectified-linear units, for which semi-analytical results are known from
 70 a computational neuroscience [12] and a machine learning [33] perspective.

71 2.2 Algebraic geometry of the equilibrium points

72 A study of the set of equilibrium points of a state-space model, $\mathcal{S}_0(\mathbf{x}) \equiv \{\mathbf{s} \ni F_{1:N}(\mathbf{s}, \mathbf{x}) = \mathbf{0}\}$,
 73 can not only help in characterising the stable equilibrium-points $\hat{\mathbf{s}} \in \mathcal{S}_* \subseteq \mathcal{S}_0$, but also provide
 74 necessary (but not sufficient) conditions in the parameters defining the functions $F_{1:N}$ and G , to
 75 realize desired equilibrium-point functionality $y(\mathbf{x})$. For example, to realize a Boolean function
 76 $y : \{0, 1\}^N \rightarrow \{0, 1\}$, the following property has to be satisfied:

$$\min_{\mathbf{s} \in \mathcal{S}_0(\mathbf{x})} G(\mathbf{s}) \leq 1 \wedge \max_{\mathbf{s} \in \mathcal{S}_0(\mathbf{x})} G(\mathbf{s}) \geq 0 \forall \mathbf{x} \in \{0, 1\}^N. \quad (3)$$

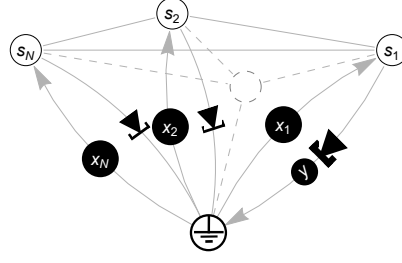


Figure 1: Recurrent physical network corresponding to the state-space model (2) where the inputs $x_{1:N}$ are currents, the states $s_{1:N}$ are voltages, the output y is a measured current, the linear interactions are due to resistors with a conductance f_{ij} between node i and j , and nonlinear interactions are due to tunnel diodes from node i to GND with conductance $G_i(s_i)$.

77 The set of equilibrium points of our recurrent physical network model (2) are the roots of the system
 78 of nonlinear equations

$$-f_{i,1:N} \cdot s_{1:N} + G_i(s_i) = x_i \quad (4)$$

79 where the linear-interaction matrix $f_{N \times N}$ has terms $f_{ii} \equiv -\sum_{j \neq i} f_{ij}$.

80 Solving the multivariate nonlinear equation (4) is a difficult problem in algebraic geometry, a
 81 discipline of mathematics which classically grew around efforts to understand the roots of multivariate
 82 polynomials and later metamorphosed by the study of integer-coefficient piecewise-linear functions,
 83 with an abstract language that has even recently been applied to explain circuit complexity results of
 84 deep feedforward networks [35, 30] through the lens of rational piecewise-linear functions [40].

85 Algebraic geometry originally dealt with a qualitative approach by geometrical arguments [15], in
 86 contrast to a quantitative approach by numerical methods. An example of that kind is Harnack's
 87 curve theorem [19] which states that for a 2-D polynomial curve of degree n , the maximum number
 88 of connected components is $(n^2 - 3n + 4)/2$. Now, with the advent of computer algebra, the roots
 89 of multivariate nonlinear equations are studied by the elimination of variables, using techniques
 90 such as resultants [13, 38] and Groebner bases [7, 8] for polynomial systems, and as an instance
 91 of the linear-complementarity problem [11] or equivalently as absolute-value equations [26] for
 92 piecewise-linear systems [37]. However, computer algebra is not scalable for higher dimensions.
 93 Thus there is a need to convey the richness in algebraic geometry using analytical expressions. While
 94 it is unlikely that analytical expressions may be obtained for any general form of nonlinearity, we
 95 may hope that the set of exactly solvable models can be extended well beyond linear equations, a
 96 hope banking on our successful experience from other areas of mathematics such as integral calculus
 97 [9, section IX] and iterated mappings [39, page 1098].

98 2.2.1 Piecewise-linear algebra

99 In this paper, we commit to a piecewise-linear analysis by considering

$$G_i(s) = \begin{cases} g_{i1}s & 0 \leq s \leq g_{i2} \\ (g_{i1} + g_{i3})g_{i2} - g_{i3}s & g_{i2} \leq s \leq g_{i2}(1 + \frac{g_{i1}}{g_{i3}}) \end{cases}, \quad (5)$$

100 where $g_{i1,2,3} > 0$ so that G_i is a triangular peak function in a limited range of s , thus defining
 101 an idealized negative-differential behaviour. Shifting the state-space about its inflection points as
 102 $z \equiv s - g_2$ and then combining (5) with (4) yields

$$x_i = \begin{cases} -f_{i,1:N} \cdot z + g_{i1}z_i - f_{i,1:N} \cdot g_2 + g_{i1}g_{i2} & -g_{i2} \leq z_i \leq 0 \\ -f_{i,1:N} \cdot z - g_{i3}z_i - f_{i,1:N} \cdot g_2 + g_{i1}g_{i2} & 0 \leq z_i \leq g_{i2}(\frac{g_{i1}}{g_{i3}}) \end{cases}, \quad (6)$$

103 which can be simplified to

$$x_i = -f_{i,1:N} \cdot z + g_{i\ominus}z_i - g_{i\oplus}|z_i| - f_{i,1:N} \cdot g_2 + g_{i1}g_{i2} \quad (7)$$

104 for $-g_{i2} \leq z_i \leq g_{i2}(\frac{g_{i1}}{g_{i3}})$ with $g_{i\ominus} \equiv (g_{i1} - g_{i3})/2$ and $g_{i\oplus} \equiv (g_{i1} + g_{i3})/2$.

105 The system in (7) can be expressed in the absolute-value equation normal form

$$\mathbf{A}\mathbf{z} - |\mathbf{z}| = \mathbf{b} \quad (8)$$

106 with $A_{ij} = (-f_{ij} + \mathbf{I}_{ij} g_{i\ominus})/g_{i\oplus}$, $b_i = (x_i + f_{i,1:N} \cdot \mathbf{g}_2 + g_{i1}g_{i2})/g_{i\oplus}$ and the bounds

$$-g_2 \leq z \leq g_2g_1/g_3. \quad (9)$$

107 Similarly, (2) can be expressed as

$$\tau \dot{z} = \mathbf{g}_{\oplus}(\mathbf{b} - \mathbf{A}\mathbf{z} + |\mathbf{z}|). \quad (10)$$

Two sufficient conditions are known for the absolute value equation (8) to have a unique solution based on the largest singular value σ_{\min} [26] and the spectral radius ρ [32]:

$$\sigma_{\min}(\mathbf{A}) > 1, \quad (11)$$

$$\rho(|\mathbf{A}^{-1}|) < 1. \quad (12)$$

108 However, those are not yet sufficient conditions for a unique equilibrium-point solution for (2) and
 109 (10) because the bounds in (9) were not enforced. Thus, we shall proceed to obtain a Lyapunov
 110 function to guarantee that a stable equilibrium-point is reached.

111 2.3 Lyapunov stability analysis

112 Equilibrium-point stability for large complex systems is not guaranteed in general [17, 27], and the
 113 effective dimensionality of stable-input stable-output responses is richly dependent on the parameter
 114 space [2]. However, the interaction matrix for our physical system (2) is symmetric, and hence the
 115 system is a special case of the Cohen-Grossberg model [10]

$$\dot{s}_i = a_i(s_i)[b_i(s_i) - \sum_{j=1}^N c_{ij}d_j(s_j)], \quad (13)$$

with $a_i(s_i) = 1/\tau_i$, $b_i(s_i) = x_i - G_i(s_i)$, $c_{ij} = -f_{ij}$ and $d_j(s_j) = s_j$. Thus, it is known to be
 globally absolute stable, with a Lyapunov function

$$V = -\sum_i \int_0^{s_i} b_i(u)d'_i(u) du + \sum_{i,j} \frac{c_{ij}}{2} d_i(s_i)d_j(s_j) \quad (14)$$

$$= \sum_i \left(P_i(s_i) - x_i s_i - \sum_{j>i} f_{ij} s_i s_j - \frac{f_{ii}}{2} s_i^2 \right), \quad (15)$$

$$\text{where output power } P_i(s_i) \equiv \int_0^{s_i} G_i(u) du. \quad (16)$$

116 Alternatively, since our system (5) is piecewise-linear, a piecewise-quadratic Lyapunov function may
 117 be obtained by a piecewise-affine system [22] analysis. While this approach is more powerful and
 118 holds even for asymmetric interaction matrices, it also seems to be analytically complex. From another
 119 angle, global asymptotic stability [21, Theorem 3] is guaranteed if the Jacobian matrix \mathbf{J} satisfies
 120 $J_{ii} + 1/2 \sum_{j \neq i} |J_{ij} + J_{ji}| < 0 \iff G'_i(s_i) > 0$ because in our system $J_{ii} = -\sum_{j \neq i} f_{ij} - G'_i(s_i)$
 121 and $J_{ij} = f_{ij}$. Since our network employs non-monotonic functionality, $G'_i(s_i) > 0$ cannot be
 122 guaranteed for all reachable states s_i , and thus the above criteria is unfortunately inapplicable. Hence,
 123 we shall proceed with the Cohen-Grossberg approach.

124 The power function (21) simplifies to

$$P(s) = \begin{cases} \int_0^s g_1 u du = g_1 s^2/2 & 0 \leq s \leq g_2 \\ g_1 g_2^2/2 + \int_{g_2}^s (g_1 + g_3)g_2 - g_3 u du & g_2 \leq s \\ = g_1 s^2/2 - g_{\oplus}(s - g_2)^2, & \end{cases} \quad (17)$$

125 and using the rectifier function $[x] \equiv \max(x, 0)$ may be expressed conveniently as

$$P(s) = g_1 s^2/2 - g_{\oplus}[s - g_2]^2, \quad (18)$$

126 when the system is within its operational bounds.

127 3 Results

128 Given the Lyapunov stability result of our system, it is computationally efficient to simulate our
129 state-space model and probe for combinational functionality. Here, we will simulate for the simplest
130 proof-of-concept for deep functionality in a shallow recurrent - solving a parity problem.

131 Using a cascade of 2-input XOR gates, the N -bit parity function can be realized with $N/2 + N/4 +$
132 $\dots + 1 = N - 1$ gates and $2N - 1$ connections. Thus its total cost in area is at least $3N - 2$ units.
133 A minimally-connected network has N input wires, 1 output wire, and $N - 1$ interconnect wires
134 with a total area cost of $2N$ units, assuming that the area occupied by the remaining components is
135 negligible. Thus for $N = 3$, while a conventional digital circuit costs 7 units, our recurrent physical
136 network takes just 6 wiring units.

137 Our simple model has $N = 3$, $f_{12} = f_{13} = f$, $f_{23} = 0$, $g_{11} = g_1$, $g_{13} = g_3$, $g_{21} = g_{31} = \gamma_1$,
138 $g_{23} = g_{33} = \gamma_3$, $g_{12} = g_2$ and $\gamma_{22} = \gamma_{32} = \gamma_2$. We find from a symbolic evaluation that $\sigma_{\min}(\mathbf{A}) \neq$
139 $1/\rho(|\mathbf{A}^{-1}|)$ in general, and conditions for unique stability were not obtainable (which is not surprising
140 due to the $s_2 - s_3$ symmetry). Thus, parity functionality was found by trial-and-error yielding the
141 parameters $\{f = 1.751, g_1 = 1.876, g_2 = g_3 = 0.126, \gamma_1 = 0.876, \gamma_2 = 1.6, \gamma_3 = 0.751\}$ and
142 simulated using Wolfram Mathematica 13 (code in Appendix). When $x_1 = x_2 = x_3 = 1$, the states
143 were forced to transition beyond the bounds in (5), so its range was extended by taking an absolute
144 value. The results are plotted in Fig. 2.

145 4 Discussion

146 Our result should be seen as a theoretical proof-of-concept and as a motivation for continued
147 research in this area. Future work must extend our simulations to much higher dimensions to serve
148 as a practical demonstration of deep functionality by shallow recurrent networks. Moreover, the
149 theoretical formalism introduced here is not yet fully exploited. We hope to find an analytical method
150 to design functionality out of piecewise-linear Cohen-Grossberg networks.

151 Our style of reasoning to circumvent the Shannon bottleneck may also be applied to other systems
152 such as networks of coupled oscillators [28]. Our non-modular mode of signal processing, offers
153 an alternative to not just circuit designers, but also to systems biologists who typically understand
154 chemical reaction networks [6] as a composition of modules [20]. While, we have discussed
155 equilibrium-point functionality in a state-space model driven by an additive input, it is also worth
156 investigating autonomous systems where the input is set as an initial state. An example is realizing
157 unboundedly-finite parity functions using just a radius-4 cellular automaton [4]. Finally, we hope
158 that this paper can serve as a call to action for neuromorphic engineers to look at physical reservoir
159 computing [36] from another angle, besides temporal input-output functionality.

160 References

- 161 [1] M. A. Alcorn, Q. Li, Z. Gong, C. Wang, L. Mai, W.-S. Ku, and A. Nguyen. Strike (with) a pose:
162 Neural networks are easily fooled by strange poses of familiar objects. In *Proceedings of the*
163 *IEEE/CVF Conference on Computer Vision and Pattern Recognition*, pages 4845–4854, 2019.
- 164 [2] R. D. Beer. Parameter space structure of continuous-time recurrent neural networks. *Neural*
165 *computation*, 18(12):3009–3051, 2006.
- 166 [3] N. Bernstein. The co-ordination and regulation of movements. *The co-ordination and regulation*
167 *of movements*, 1966.
- 168 [4] H. Betel, P. P. de Oliveira, and P. Flocchini. Solving the parity problem in one-dimensional
169 cellular automata. *Natural Computing*, 12(3):323–337, 2013.
- 170 [5] E. Bizzi, N. Hogan, F. A. Mussa-Ivaldi, and S. Giszter. Does the nervous system use equilibrium-
171 point control to guide single and multiple joint movements? *Behavioral and brain sciences*,
172 15(4):603–613, 1992.

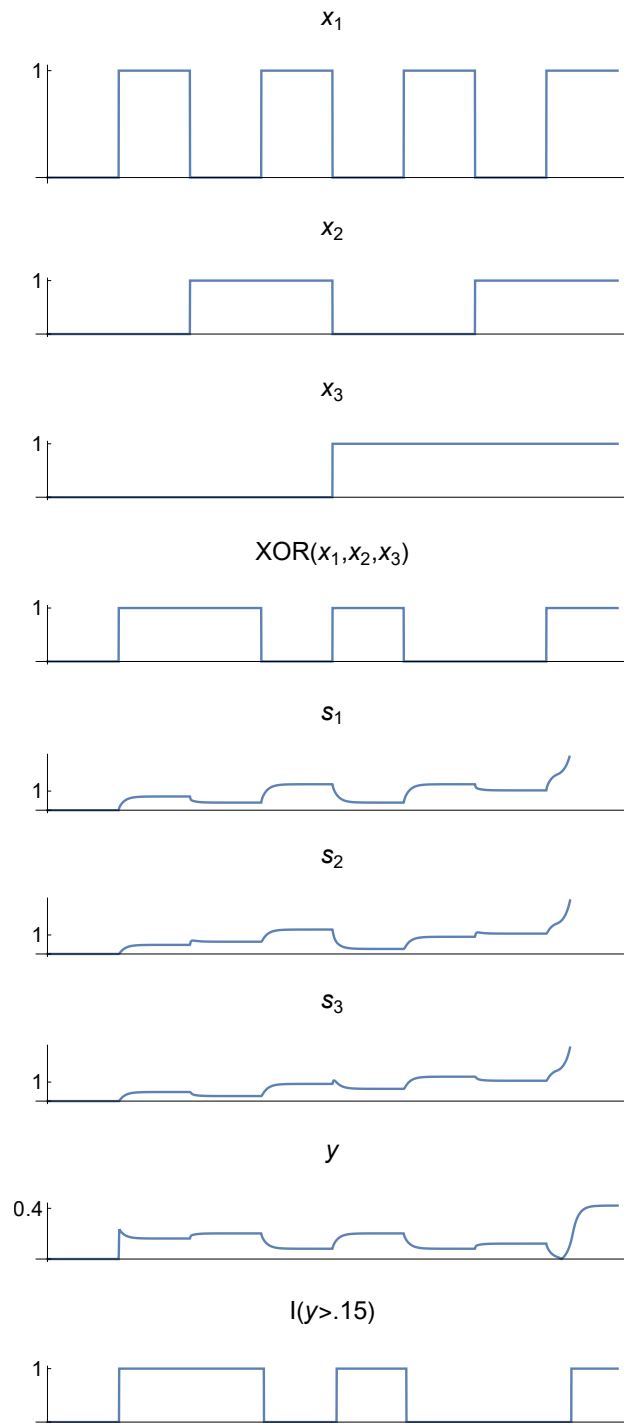


Figure 2: Numerical simulation of our 3-state network over 200 timesteps.

- 173 [6] D. Bray. Protein molecules as computational elements in living cells. *Nature*, 376(6538):307–
174 312, 1995.
- 175 [7] B. Buchberger. Ein algorithmus zum auffinden der basiselemente des restklassenringes nach
176 einem nulldimensionalen polynomideal. *PhD thesis, Universitat Insbruck*, 1965.
- 177 [8] B. Buchberger. Bruno buchberger’s phd thesis 1965: An algorithm for finding the basis
178 elements of the residue class ring of a zero dimensional polynomial ideal. *Journal of symbolic*
179 *computation*, 41(3-4):475–511, 2006.
- 180 [9] G. S. Carr. Synopsis of elementary results in pure mathematics. 1886.
- 181 [10] M. A. Cohen and S. Grossberg. Absolute stability of global pattern formation and parallel
182 memory storage by competitive neural networks. *IEEE transactions on systems, man, and*
183 *cybernetics*, (5):815–826, 1983.
- 184 [11] R. W. Cottle. *Linear complementarity problem*, pages 1873–1878. Springer US, Boston, MA,
185 2009.
- 186 [12] D. Durstewitz. A state space approach for piecewise-linear recurrent neural networks for
187 identifying computational dynamics from neural measurements. *PLoS computational biology*,
188 13(6):e1005542, 2017.
- 189 [13] I. Z. Emiris. On the complexity of sparse elimination. *Journal of Complexity*, 12(2):134–166,
190 1996.
- 191 [14] A. G. Feldman. Functional tuning of the nervous system with control of movement or main-
192 tenance of a steady posture-ii. controllable parameters of the muscle. *Biofizika*, 11:565–578,
193 1966.
- 194 [15] W. Fulton. *Intersection theory*, volume 2. Springer Science & Business Media, 2013.
- 195 [16] S. Gao, M. Zhou, Y. Wang, J. Cheng, H. Yachi, and J. Wang. Dendritic neuron model with ef-
196 fective learning algorithms for classification, approximation, and prediction. *IEEE transactions*
197 *on neural networks and learning systems*, 30(2):601–614, 2019.
- 198 [17] M. R. Gardner and W. R. Ashby. Connectance of large dynamic (cybernetic) systems: critical
199 values for stability. *Nature*, 228(5273):784–784, 1970.
- 200 [18] I. J. Goodfellow, J. Shlens, and C. Szegedy. Explaining and harnessing adversarial examples,
201 2015.
- 202 [19] A. Harnack. Ueber die vieltheiligkeit der ebenen algebraischen curven. *Mathematische Annalen*,
203 10(2):189–198, 1876.
- 204 [20] L. H. Hartwell, J. J. Hopfield, S. Leibler, and A. W. Murray. From molecular to modular cell
205 biology. *Nature*, 402(6761):C47–C52, 1999.
- 206 [21] M. W. Hirsch. Convergent activation dynamics in continuous time networks. *Neural networks*,
207 2(5):331–349, 1989.
- 208 [22] M. Johansson and A. Rantzer. Computation of piecewise quadratic lyapunov functions for
209 hybrid systems. In *1997 European Control Conference (ECC)*, pages 2005–2010. IEEE, 1997.
- 210 [23] J. Kubilius, M. Schrimpf, K. Kar, R. Rajalingham, H. Hong, N. Majaj, E. Issa, P. Bashivan,
211 J. Prescott-Roy, K. Schmidt, et al. Brain-like object recognition with high-performing shallow
212 recurrent anns. *Advances in neural information processing systems*, 32, 2019.
- 213 [24] C. P. Lawrence. *Evolving Networks To Have Intelligence Realized At Nanoscale*. PhD thesis,
214 University of Twente, 2018.
- 215 [25] M. Liang and X. Hu. Recurrent convolutional neural network for object recognition. In
216 *Proceedings of the IEEE conference on computer vision and pattern recognition*, pages 3367–
217 3375, 2015.

- 218 [26] O. Mangasarian and R. Meyer. Absolute value equations. *Linear Algebra and Its Applications*,
219 419(2-3):359–367, 2006.
- 220 [27] R. M. May. Will a large complex system be stable? *Nature*, 238(5364):413–414, 1972.
- 221 [28] S. N. Menon and S. Sinha. “defective” logic: Using spatiotemporal patterns in coupled relaxation
222 oscillator arrays for computation. In *2014 International Conference on Signal Processing and*
223 *Communications (SPCOM)*, pages 1–6. IEEE, 2014.
- 224 [29] S.-M. Moosavi-Dezfooli, A. Fawzi, O. Fawzi, and P. Frossard. Universal adversarial pertur-
225 bations. In *Proceedings of the IEEE conference on computer vision and pattern recognition*,
226 pages 1765–1773, 2017.
- 227 [30] M. Raghu, B. Poole, J. Kleinberg, S. Ganguli, and J. Sohl-Dickstein. On the expressive power
228 of deep neural networks. In *international conference on machine learning*, pages 2847–2854.
229 PMLR, 2017.
- 230 [31] M. D. Riedel and J. Bruck. Cyclic boolean circuits. *Discrete Applied Mathematics*, 160(13-
231 14):1877–1900, 2012.
- 232 [32] J. Rohn, V. Hooshyarbakhsh, and R. Farhadsefat. An iterative method for solving absolute value
233 equations and sufficient conditions for unique solvability. *Optimization Letters*, 8(1):35–44,
234 2014.
- 235 [33] D. Schmidt, G. Koppe, Z. Monfared, M. Beutelspacher, and D. Durstewitz. Identifying nonlinear
236 dynamical systems with multiple time scales and long-range dependencies. In *International*
237 *Conference on Learning Representations*, 2021.
- 238 [34] C. E. Shannon. The synthesis of two-terminal switching circuits. *The Bell System Technical*
239 *Journal*, 28(1):59–98, 1949.
- 240 [35] K.-Y. Siu, V. P. Roychowdhury, and T. Kailath. Depth-size tradeoffs for neural computation.
241 *IEEE Transactions on Computers*, 40(12):1402–1412, 1991.
- 242 [36] G. Tanaka, T. Yamane, J. Héroux, R. Nakane, N. Kanazawa, S. Takeda, H. Numata, D. Nakano,
243 and A. Hirose. Recent advances in physical reservoir computing: A review. *Neural Networks*,
244 115:100–123, 2019.
- 245 [37] W. M. Van Bokhoven and D. M. Leenaerts. Explicit formulas for the solutions of piecewise
246 linear networks. *IEEE Transactions on Circuits and Systems I: Fundamental Theory and*
247 *Applications*, 46(9):1110–1117, 1999.
- 248 [38] M. P. Williams. Solving polynomial equations using linear algebra. *Johns Hopkins APL*
249 *Technical Digest*, 28(4):354–363, 2010.
- 250 [39] S. Wolfram. *A new kind of science*, volume 5. Wolfram media Champaign, IL, 2002.
- 251 [40] L. Zhang, G. Naitzat, and L.-H. Lim. Tropical geometry of deep neural networks. In *Interna-*
252 *tional Conference on Machine Learning*, pages 5824–5832. PMLR, 2018.

253 Checklist

- 254 1. For all authors...
- 255 (a) Do the main claims made in the abstract and introduction accurately reflect the paper’s
256 contributions and scope? [Yes] The concrete result is the realization of a parity function
257 by our recurrent physical network by using just 6 wiring units, while a conventional
258 digital circuit costs 7 units. That being said, the paper is written to cover a much
259 broader scope - this is a matter of taste (an earlier version of this manuscript recieved
260 both positive and negative comments about the scope of this article).

- 261 (b) Did you describe the limitations of your work? [Yes] It is mentioned that future
 262 work must extend our simulations to much higher dimensions to serve as a practical
 263 demonstration of deep functionality by shallow recurrent networks. Also the simulation
 264 parameters were found by trial and error, instead of being derived analytically from the
 265 theoretical formalism - these limitations are mentioned in the discussion.
- 266 (c) Did you discuss any potential negative societal impacts of your work? [N/A]
- 267 (d) Have you read the ethics review guidelines and ensured that your paper conforms to
 268 them? [Yes]
- 269 2. If you are including theoretical results...
- 270 (a) Did you state the full set of assumptions of all theoretical results? [N/A]
- 271 (b) Did you include complete proofs of all theoretical results? [N/A]
- 272 3. If you ran experiments...
- 273 (a) Did you include the code, data, and instructions needed to reproduce the main ex-
 274 perimental results (either in the supplemental material or as a URL)? [Yes] Check
 275 Appendix for the code to reproduce Figure 2.
- 276 (b) Did you specify all the training details (e.g., data splits, hyperparameters, how they
 277 were chosen)? [N/A]
- 278 (c) Did you report error bars (e.g., with respect to the random seed after running experi-
 279 ments multiple times)? [N/A]
- 280 (d) Did you include the total amount of compute and the type of resources used (e.g., type
 281 of GPUs, internal cluster, or cloud provider)? [N/A] It is evident that Figure 2 is not a
 282 large-scale deep learning experiment but a small-scale conceptual simulation which
 283 takes less than 2 seconds on a modern desktop CPU.
- 284 4. If you are using existing assets (e.g., code, data, models) or curating/releasing new assets...
- 285 (a) If your work uses existing assets, did you cite the creators? [N/A]
- 286 (b) Did you mention the license of the assets? [N/A]
- 287 (c) Did you include any new assets either in the supplemental material or as a URL? [No]
- 288 (d) Did you discuss whether and how consent was obtained from people whose data you're
 289 using/curating? [N/A]
- 290 (e) Did you discuss whether the data you are using/curating contains personally identifiable
 291 information or offensive content? [N/A]
- 292 5. If you used crowdsourcing or conducted research with human subjects...
- 293 (a) Did you include the full text of instructions given to participants and screenshots, if
 294 applicable? [N/A]
- 295 (b) Did you describe any potential participant risks, with links to Institutional Review
 296 Board (IRB) approvals, if applicable? [N/A]
- 297 (c) Did you include the estimated hourly wage paid to participants and the total amount
 298 spent on participant compensation? [N/A]

299 A Appendix

300 Wolfram Mathematica code to reproduce Figure 2.

```

301 In[ ]:= simulate[f_, g_, γ_] := (sys = NonlinearStateSpaceModel[{
  {x1 - (2 f) s1 + f (s2 + s3) - Abs[g[[1]] * s1 - (g[[1]] + g[[3])] Ramp[s1 - g[[2]]],
  x2 - (f) s2 + f (s1) - Abs[γ[[1]] s2 - (γ[[1]] + γ[[3])] Ramp[s2 - γ[[2]]],
  x3 - (f) s3 + f (s1) - Abs[γ[[1]] s3 - (γ[[1]] + γ[[3])] Ramp[s3 - γ[[2]]]},
  {x1, x2, x3, Xor[x1, x2, x3], s1, s2, s3, y = Abs[g[[1]] s1 - (g[[1]] + g[[3])] Ramp[s1 - g[[2]]], HeavisideTheta[y - .15]}
}, {s1, s2, s3}, {x1, x2, x3}];
  inputs = {.5 - .5 * SquareWave[t / 50], .5 - .5 * SquareWave[t / 100], .5 - .5 * SquareWave[t / 200]};
  out = OutputResponse[{sys, {0, 0}}, inputs, {t, 0, 200}];
  GraphicsColumn@Table[Plot[out[[i]], {t, 0, 200}, PlotRange -> All, Ticks -> {Automatic, {0, 1/5, 1, 2}}, {i, 9}]]
  simulate[1.751, {1.876, .126, .126}, {.876, 1.6, .751}]

```